ФИЗИКА ПРОЧНОСТИ И ПЛАСТИЧНОСТИ

Effect of Liquid Salt Bath Nitrocarburizing on Mechanical Properties of Low-Alloy Sintered Steels

S. Serrai, S. Mechachti, O. Benchiheub, S. Boudebane[*], M. Fellah[**], and M. Z. Touhami

*Badji Mokhtar University,
Laboratory of Research in Foundry,
Department of Metallurgy and Materials Engineering,
BO 12, CP 23000 Annaba, Algeria*
[*]*Badji Mokhtar University,
Laboratory of Metallurgy and Material Engineering,
BO 12, CP 23000 Annaba, Algeria*
[**]*Badji Mokhtar University,
Tribology, Materials Surface and Interfaces Group, Laboratory of Foundry,
BO 12, CP 23000 Annaba, Algeria*

The purpose of this study is to produce $Fe-2Cu-2Ni-0.7Mo-XC$ steels by means of the powder metallurgy at different sintering temperatures. The mechanical properties of sintered steels have recently reached a level equivalent to that of steels produced by other processes. The static and dynamic mechanical properties of parts made of sintered steel depend on density and microstructure. Many process parameters such as initial composition, alloying elements, atmosphere, time, sintering temperature, and nitrocarburizing influence the microstructure of steel parts. The compacts' preparation involves powder mixing, cold pressing at 500 MPa, and sintering at 1250°C within the H_2 atmosphere for 2 hours and 25 min. The influence of sintering temperature on both hardness and microstructure of the steel is investigated. In this study, sintered $Fe-2Cu-2Ni-0.7Mo-XC$-type steels are developed. The impact of nitrocarburizing on this structure is evaluated. Microscopy, SEM, and destructive testing are used for characterization of the sintered steels.

Corresponding author: Salim Serrai
E-mail: salimredha_206@yahoo.fr

Метою даної роботи є одержання сталей типу Fe−2Cu−2Ni−0,7Mo−XC методами порошкової металурґії за різних температур спікання. Механічні властивості спечених сталей нещодавно сягнули рівня, аналогічного рівню сталей, що виробляються іншими методами. Статичні та динамічні механічні властивості деталів із спеченої сталі визначаються густиною та мікроструктурою. При цьому велика кількість характеристик процесу, наприклад, вихідний склад, леґувальні елементи, атмосфера, час, температура спікання та нітроцементація впливають на мікроструктуру сталевих деталів. Виготовлення пресованого матеріялу потребує змішування порошку, холодного пресування при 500 МПа та спікання при температурі у 1250°С в атмосфері H$_2$ протягом 2 годин 25 хв. Було досліджено вплив температури спікання на твердість і мікроструктуру сталі. В даній роботі було розглянуто сталі типу Fe−2Cu−2Ni−0,7Mo−XC. Було проведено оцінку впливу нітроцементації на такі структури. Для характеризації спечених сталей використовувалися мікроскопія, СЕМ та випробування на руйнування.

Ключові слова: мікроструктура, нітроцементація, леґувальні елементи, пористість, густина, мікротвердість.

Целью данной работы является получение сталей типа Fe−2Cu−2Ni−0,7Mo−XC методами порошковой металлургии при различных температурах спекания. Механические свойства спечённых сталей недавно достигли уровня, аналогичного уровню сталей, производимых другими методами. Статические и динамические механические свойства деталей из спечённой стали определяются плотностью и микроструктурой. При этом большое количество характеристик процесса, например, исходный состав, легирующие элементы, атмосфера, время, температура спекания и нитроцементация, влияют на микроструктуру стальных деталей. Изготовление прессованного материала требует смешивания порошка, холодного прессования при 500 МПа и спекания при температуре 1250°С в атмосфере H$_2$ в течение 2 часов 25 мин. Было исследовано влияние температуры спекания на твёрдость и микроструктуру стали. В данной работе были рассмотрены стали типа Fe−2Cu−2Ni−0,7Mo−XC. Была проведена оценка влияния нитроцементации на такие структуры. Для характеризации спечённых сталей использовались микроскопия, СЭМ и испытания на разрушение.

Ключевые слова: микроструктура, нитроцементация, легирующие элементы, пористость, плотность, микротвёрдость.

1. INTRODUCTION

Powder metallurgy (PM) production method of steel parts with complex shape is cheaper comparing to other manufacturing methods [1].

PM has advanced significantly over the past 30 years as a cost effective and efficient processing technique to produce near net shape parts [2]. PM is often used when it comes to developing materials, which are not easily developed by conventional melting processes. Metal matrix composites reinforced by dispersing various reinforcements (carbides, oxides, nitrides, intermetallics) are one such class of materials, which are developed by powder metallurgy.

New powder metallurgy materials having high performance have been required due to necessity in various industrial applications. There are many ways to increase the performance of materials including new alloy systems, increasing the density by using new compaction techniques, increasing sintering temperature, and heat treatments. Pre-alloyed diffusion powders have been developed in order to obtain high-performance materials [3−5].

Many performance-enhancing pre-alloying elements such as molybdenum, manganese, nickel, and chromium have been used. The low-alloy sintered Fe−Ni−Cu−Mo−C steel has a great attention of several researchers [4, 6−10]. With the introduction of graphite into the iron powder, it is possible to obtain ferrous sintered materials having different structures and properties. Moreover, it improves the sintering behaviour, and a high content of graphite leads to a better dissemination.

Nickel is one of the most important alloying elements in steels, and it can be used in ferrous alloys in low-alloy powders [11−14]. Addition of 0.5 to 5% of nickel increases tensile strength and ductility, whereas adding molybdenum produces a finer structure and improves its performance and mechanical properties [11−14].

To be considered for high-performance applications, powder metallurgy materials must have a reduced porosity and an enhanced density. To achieve this one, various techniques have been used during the production process of these materials. Employing high sintering temperature is an alternative way to produce PM materials with desired microstructural and mechanical properties.

The success of manufacturing techniques associated with powder metallurgy undoubtedly lies in the productivity rates, which can never be matched especially for shaping metal parts with complex geometries. For some categories of parts, powder metallurgy stands as a quality alternative to the more conventional methods such as casting, forging, and machining. Powder metallurgy enables substantial savings by eliminating rework machining.

2. EXPERIMENTAL DETAILS

Table 1 shows the chemical composition, particle size, and properties of hydrogen-reduced iron of the two mixtures used in this study, mixture 1 (2% Cu, 2% Ni, 0.7% Mo, and 0.4% C) and mixture 2 (2% Cu,

TABLE 1. Chemical composition and properties of the reduced iron powder.

Chemical composition (mass fraction), %	
C	≤ 0.04
O	≤ 0.4
Fe	Balance
Theoretical density, g/cm^3	7.84
Bulk density, g/cm^3	1.73
Size distribution of particles, %	
≤ 45	59.40
$45-106$	39.30
$106-150$	1.30
> 150	0.5

2% Ni, 0.7% Mo, and 0.6% C). These mixtures are then mixed with the starting iron powder. The powder elements origins and sizes are as follows: reduced iron (50 µm), nickel carbonyl (10 µm), reduced copper (< 90 µm), reduced molybdenum (< 2.61 µm) and graphite ($1-2$ µm).

In order to achieve a homogeneous mixture of powders of Fe, C, Cu, Ni, and Mo, we used a ball mill for 10 hours. A synthetic wax was then added at 100 ml/kg of powder to act as a lubricant during the compacting operation and to increase the green density thus improving the resistance of the parts after compaction and facilitating their handling prior to sintering [15]. Then, the mixture thereof is heated in an oven at a temperature of about 300°C.

The lubricant added to the load reduces friction couples (particle/particle) and (particle/wall) during compression, thus ensuring the better transmission of stresses within the volume occupied by the powder, which reduces density differences in the obtained agglomerates. The samples are compacted by a 1000 kN nominal pressure hydraulic press with axial compression.

For characterization, the sintered alloy steel samples were compacted under a pressure of 500 MPa. Mechanical tests were carried out using ISO standard specimens. Their dimensions were $90 \times 18 \times 5$ mm^3 for traction [16], $55 \times 10 \times 10$ mm^3 for resilience [17], and $30 \times 5 \times 5$ mm^3 for flexion [18].

After preliminary testing, we opted for sintering at high temperature (1250°C for 2 hours 25 min) in a hydrogen-reducing atmosphere in order to remove the oxides present on the grain surface and its protection from subsequent oxidation during sintering and cooling.

Liquid nitrocarburizing treatment process was performed at 580°C for 3 hours in an industrial molten salt bath consisting of 60% KCN,

TABLE 2. Green and sintered densities.

Steels	Green density, g/cm^3	Sintered density, g/cm^3
Fe0.4C2Cu2Ni0.7Mo	6.55	6.7
Fe0.6C2Cu2Ni0.7Mo	6.67	6.8

24% KCl and 16% K_2CO_3 by weight.

3. RESULTS AND DISCUSSION

3.1. Chemical Composition and Densities of Low-Alloy Sintered Steels

The green and sintered densities were deduced from the volume and weight measurement of the samples before and after sintering. The resulting densities are shown in Table 2.

The results obtained by x-ray fluorescence analysis are given in Table 3.

Under standard sintering conditions of low-alloy steels at a temperature of 1120°C for 30 min, the diffusion, which generally occurs in a solid state, does not allow complete homogenization of the alloying elements [19]. In our case, sintering was achieved at 1250°C during 2 hours 25 min. This allowed the carbon to diffuse completely with a homogeneous dispersion across the part.

3.2. Mechanical Properties of the Sintered and Nitrocarburized Steels

The increase in carbon content from 0.4 to 0.6% improves the tensile strength (Rm) of the sintered steel from 215 to 256 MPa and decreases the elongation from 0.9 to 0.6%. This is due to the formation of pearlite rather than ferrite [20]. This improvement was also noticed when the steels were treated in a salt bath. The tensile strength increases from 235 to 270 MPa, whereas the elongation decreases from 0.5 to 0.2%. This is due to the formation of nitrocarburized surface layers (Fig. 1), the latter tending to harden the steels (Table 4). This is also

TABLE 3. Fluorescence X chemical composition of Fe2Cu2Ni0.7MoXC sintered steel samples.

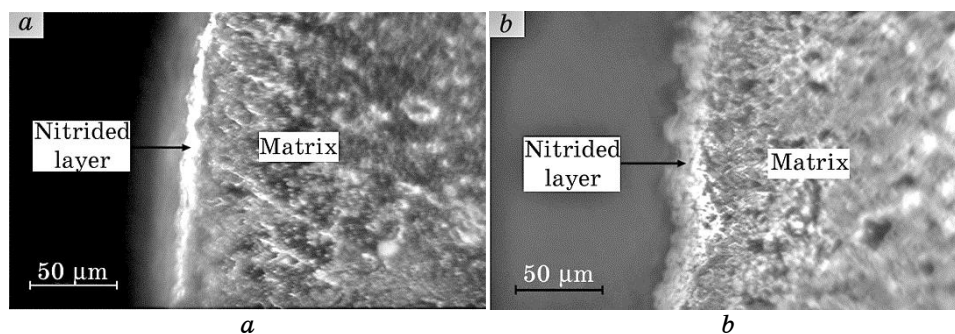| Steels	Chemical Elements, %								
	C	Ni	Cu	Mo	Si	Mn	P	V	S
Fe0.4C2Cu2Ni0.7Mo	0.4	1.985	1.852	0.742	0.928	0.159	0.012	0.018	−
Fe0.6C2Cu2Ni0.7Mo	0.6	1.973	1.310	0.710	1.063	0.125	0.029	0.017	0.0023

Fig. 1. Microstructures of nitrocarburized steels (3 hours) etched with 2% Nital: Fe0.4C2Cu2Ni0.7Mo (*a*), Fe0.6C2Cu2Ni0.7Mo (*b*).

confirmed by scanning electronic microscopy (Fig. 2).

The resilience, the resistance to flexion and the Vickers hardness of the steels were improved significantly with increasing carbon content in both sintered and nitrocarburized states. For the sintered state, they increase from 20.43 to 23.35 kJ/m^3, 898 to 1279 N/mm^2 and 235 to 239 *HV*, respectively. As shown in Table 4, for the treated steels, they increase from 43 to 47 kJ/m^3, 1046 to 1410 N/mm^2 and 245 to 247 *HV*, respectively. This is due to modification of the surface layer after nitrocarburizing. The latter promotes the formation of iron nitrides, which increase the hardness [21].

Copper promotes diffusion and improves quality of sintering bridges [22–24], thus improving hardness and increasing steel strength from 215 to 256 MPa (Table 4).

Figure 3 shows the evolution of microhardness depending on nitriding depth obtained for the two sintered and nitrocarburized steels, Fe0.4C2Cu2Ni0.7Mo and Fe0.6C2Cu2Ni0.7Mo. It shows an increase in

TABLE 4. Mechanical properties of sintered and nitrocarburized steels.

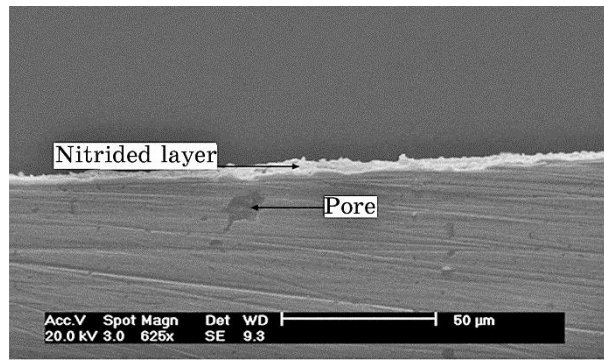| Steels	Rm, MPa	A, %	Resilience, kJ/m^3	Flexion, N/mm^2	Vickers hardness, $HV_{0.2}$
Fe0.4C2Cu2Ni0.7Mo sintered	215	0.9	20.43	898	235
Fe0.6C2Cu2Ni0.7Mo sintered	256	0.6	23.35	1279	239
Fe0.4C2Cu2Ni0.7Mo nitrocarburized	235	0.5	43	1046	245
Fe0.6C2Cu2Ni0.7Mo nitrocarburized	270	0.2	47	1410	247

Fig. 2. SEM image of the nitrocarburized steel Fe0.4C2Cu2Ni0.7Mo.

the microhardness of the nitrocarburized steel at the combination layer (Fig. 1).

This happens due to the changes in the formed phases (precipitated nitrides or carbonitrides), which are induced by the diffusion reactions of the liquid bath elements (C, N) [25].

3.3. Microstructure of Sintered and Nitrocarburized Steels

Figure 4 shows the results of the metallographic analysis of samples with varying compositions and in various states. The presence of pores
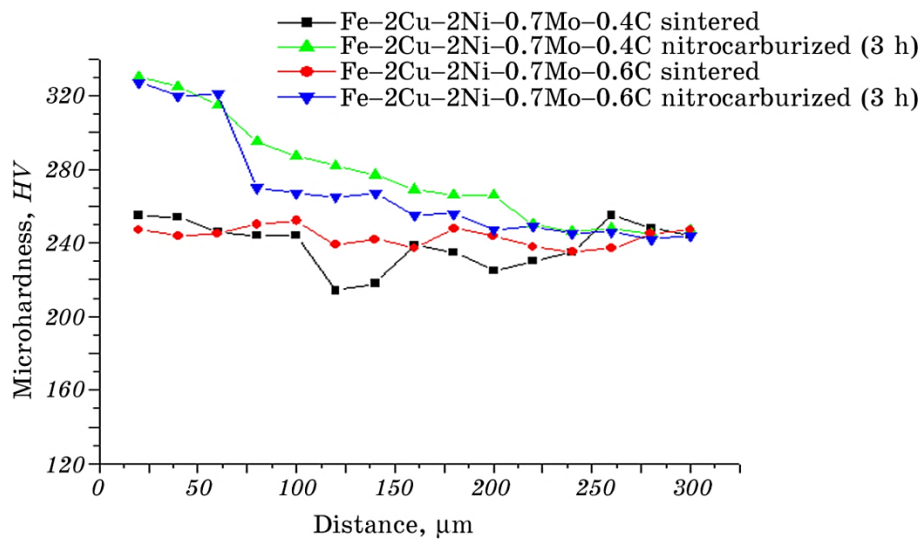

Fig. 3. Vickers microhardness profile from the surface to the centre of the sintered and the nitrocarburized steel samples.
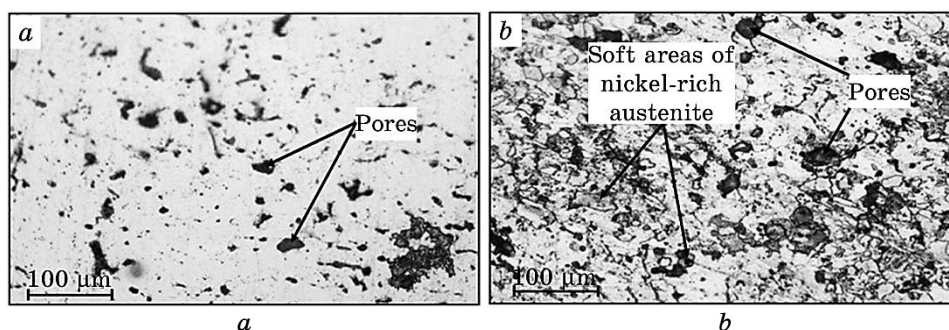
Fig. 4. Microstructures of the sintered steel Fe0.4C2Cu2Ni0.7Mo: non-etched (*a*), etched with 2% Nital (*b*), etched with 3% Nital (*c*).

is observed in the structure of the non-etched sample (Fig. 4, *a*). The enclosed pores and their spheroidization result from the progress of sintering mechanisms with a decrease of the pore volume due to the formation of phases such as ferrite, pearlite and soft areas of nickel-rich austenite (Fig. 4, *b*) [26]. The clear appearance of the grain boundaries was also observed for the entire microstructure (Fig. 4, *c*).

Figure 5 shows that the microstructures of the sintered steel Fe0.6C2Cu2Ni0.7Mo consist of pearlite, ferrite, and nickel rich austenitic ductile areas, mainly localized around the initial particles of iron powders.

3.4. X-Ray Analysis Patterns of the Nitrocarburized Layers

X-ray diffraction patterns of samples (Fig. 6) show the presence of oxides (Fe_2O_3, Fe_3O_4), cementite Fe_3C, and iron nitrides ε-$Fe_{2-3}N$ and γ'-Fe_4N. Iron oxides formed at the surface layer of the samples are a consequence of blowing oxygen in the salt bath in order to homogenize the composition and accelerate the diffusion process [27, 28]. Blowing oxygen in the salt bath is carried out periodically during the treatment. This affects the kinetics of nitriding and the composition of phases of unstable (ε-$Fe_{2-3}N$) and stable nitride (γ'-Fe_4N) [29]. The percentage of the two nitrides ε and γ' in the surface layer depends on the steel carbon content. High carbon content helps the formation of iron nitride ε-$Fe_{2-3}N$, and inversely, lower carbon content results in the appearance of γ'-Fe_4N iron nitride known for its stability.

3.5. Friction Coefficient and Wear Behaviour of Sintered and Nitrocarburized Steels

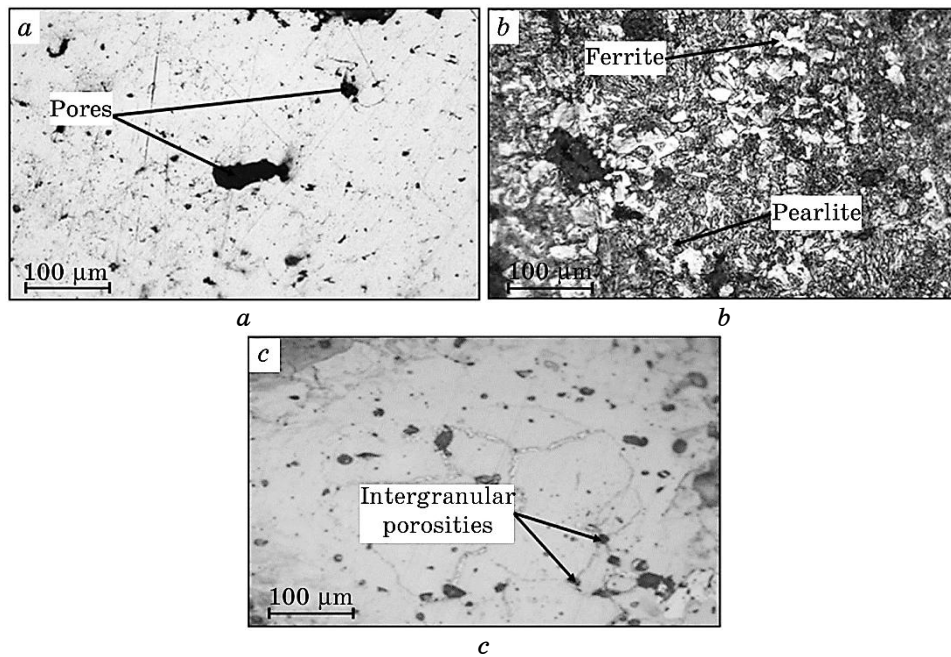The tribological behaviour of the studied materials depends on the sin-

Fig. 5. Microstructures of the sintered steel Fe0.6C2Cu2Ni0.7Mo: non-etched (*a*), etched with 2% Nital (*b*), etched with 3% Nital (*c*).

tered steels state and on the parameters of the applied thermochemical treatment [30]. Figure 7 shows the curves illustrating the evolution of the coefficient of friction over a distance of 20 m for several states. Samples sintered at 1250°C for 2 hours 25 min exhibit a similar behaviour during the first stage from 0 to 10 m, considered as a lapping step, which is characterized by a sudden increase in C_f from 0.3 to 0.55−0.65 due to crushing of surface asperities. Beyond 10 m, the surface strain hardens resulting in a stabilization of the coefficient of friction. The C_f stabilizes at 0.5 for the Fe0.4C2Cu2Ni0.7Mo sample and at 0.6 for the sample containing 0.6% C. This is explained by an increased content of free graphite in the structure; and it is known that graphitization is accelerated by the presence of elements such as Ni and Cu [31]. These elements, by their action on the thermodynamic carbon activity, promote graphitization thus creating graphite nodules, which act as lubricant. On the other hand, disturbances recorded on the curves of the sintered Fe0.4C2Cu2Ni0.7Mo and Fe0.6C2Cu2Ni0.7Mo samples confirm the existence on the surface of the εp-hardening-fragile fracture cycle.

The impact of the liquid nitrocarburizing on the sintered surface clearly appears through the values of C_f (Fig. 7, *a*). Low at the begin-
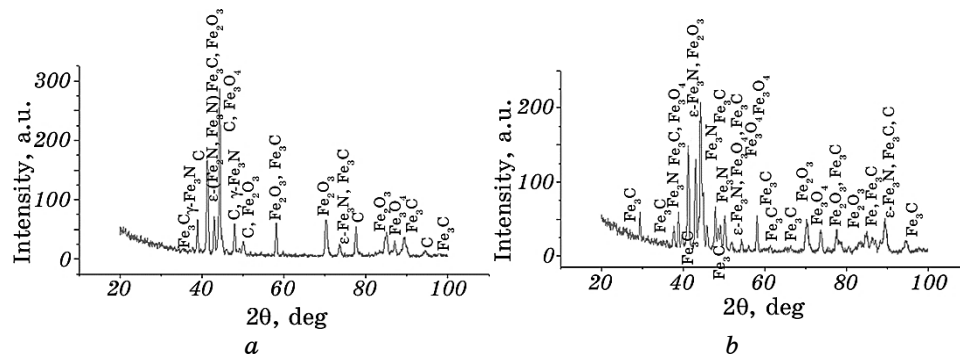
Fig. 6. X-ray diffraction diagrams ($\lambda = 1.54060$ Å) nitrocarburized steel: Fe0.4C2Cu2Ni0.7Mo (*a*), Fe0.6C2Cu2Ni0.7Mo (*b*).

ning of the test (0−5 m), the coefficient of friction of the Fe0.4C2Cu2Ni0.7Mo and Fe0.6C2Cu2Ni0.7Mo samples nitrocarburized during 3 hours, shows a monotonic increase without visible stabilization. The sample containing 0.6% C shows a strongly disturbed curve after 12 m of sliding. This phenomenon can be explained by the fragile degradation of the nitrocarburized layer and the formation of a third body (oxide or nitride particles) detached from the surface [32].

However, the sample with the lesser content carbon shows a smoother curve without visible disturbances, reflecting a deterioration by abrasion without detachment of the particles. The coefficient of friction stabilizes after 15 m without significant deterioration of the surface.
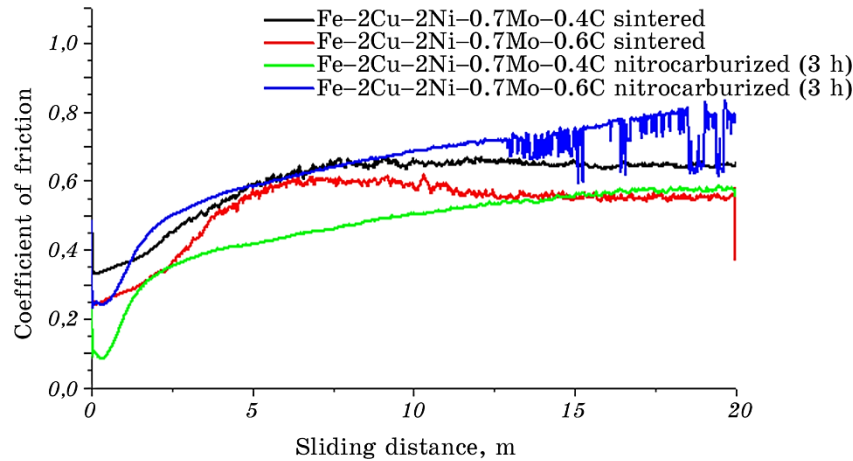

Fig. 7. Evolution of the coefficient of friction with sliding course for sintered and nitrocarburized steels.

The abrasive nature of the degradation of the surface is predominant for the nitrocarburized samples due to the presence of hard phases such as iron oxides and nitrides.

4. CONCLUSION

In this work, new sintered steels have been developed by the powder metallurgy technique under cold compaction. The structural, physical and mechanical characteristics of the morphology were studied for different compositions of these steels.

This study allowed the determination of the parameters influencing the development of low alloy sintered steels, the influence of alloying elements during the compaction process (compressibility, green density), and the effect of the carbon content on the microstructure, which in turn affects the mechanical properties of these steels. Results showed.

The minimum porosity is obtained by the use of very fine powders, with sintering at high temperature with a long hold time.

High-temperature sintering favours homogenization of the material due to a better diffusion of the alloying elements, which tend to fill the small pores, and their shrinkage.

Mechanical tests have demonstrated the influence of the microstructure on the mechanical properties of these steels.

Nitrocarburization makes it possible to modify the nature and the proportions of the formed phases, following a selective diffusion due to the solid phase diffusion reactions of the group (C, N, O).

The presence of dispersed reinforcements such as nitrocarbides, oxides and intermetallics due to the nitrocarburization can improve the hardness from 235 to 247 HV depending on the additives content of the salt bath.

The sintered samples exhibit similar wear behaviours and friction coefficients during the first step from 0 to 10 m, considered as the lapping step.

Beyond 10 m, the surface is hardened, and there is a sudden increase in C_f, which is linked to the crushing of the surface asperities.

The greater presence of free graphite in the structure and the presence of elements such as Ni and Cu, which, by their action on the thermodynamic activity of carbon, favour the graphitization by creating graphite nodules, which act as lubricant.

The very low friction coefficient observed at the beginning ($C_f = = 0.1$), increases significantly after a sliding distance of 15 m to reach 0.6 for the nitrocarburized samples.

The abrasive nature of the degradation of the surface is predominant for these samples due to the presence of hard phases such as iron oxides and nitrides.

REFERENCES

1. R. M. German, *Powder Metallurgy of Iron and Steel* (New York: John Willey and Sons: 1998).
2. K. S. Narasimhan, *Materials Chemical Physic*, **67**: 56 (2001).
3. R. J. Causton and J. J. Fulmer, *Proc. Advances in Powder Metallurgy and Particulate Materials*, **5**: 17 (1992).
4. V. A. Tracey, *Proc. Conf. on Advances in Powder Metallurgy and Particulate Materials* (Eds. A. Lawley and A. Swanson) (California, USA: 1992), vol. **5**, p. 303.
5. G. S. Upadhyaya, *Sintered Metallic and Ceramic Materials. Preparation, Properties and Applications* (New York: John Wiley and Sons: 2000).
6. H. Khorsand, S. M. Habibi, H. Yoozbashizadea, K. Janghorban, S. M. S. Reihani, H. Rahmani Seraji, and M. Ashtari, *Materials and Design*, **23,** Iss. 7: 667 (2002).
7. R. YIlmaz and A. Gökçe, *Proc. 13th International Metallurgy and Materials Congress* (Istanbul: 2006), p. 903.
8. R. YIlmaz and A. Gökçe, *Proc. 11th International Materials Symposium* (Denizli: 2006), p. 760.
9. R. YIlmaz, A. Gökçe, and H. Kapdibaú, *Advanced Materials Research, Materials and Technologies*, **22−23**: 71 (2007).
10. R. Yilmaz and Ö. Özgün, *Proc. 14 the International Metallurgy and Materials Congress* (Istanbul: 2008).
11. N. Chawla, S. Polasik, K. S. Narasimhan, T. Murphy, M. Koopman, and K. K. Chawla, *Int. J. Powder Metall.*, **37**: 49 (2001).
12. N. Chawla, T. F. Murphy, K. S. Narasimhan, M. Koopman, and K. K. Chawla, *Mater. Sci. Eng. A*, **308,** Iss. 1−2: 180 (2001).
13. N. Chawla, D. Babic, J. J. Williams, S. J. Polasik, M. Marucci, and K. S. Narasimhan, *Adv. Powder Metall. Part. Mater Metal Powder Industries Federation*, **5**: 104 (2002).
14. S. J. Polasik, J. J. Williams, and N. Chawla, *Metall. Mater. Trans. A*, **33,** Iss. 1: 73 (2002).
15. P. Lemieux, Y. Thomas, P. E. Mongeon, S. Pelletier, and S. St-Laurent, *Powder Metallurgy Technology*, 24(3): 227 (2006).
16. *Eprouvette Pour Essai de Traction*, Norme ISO 2740 (2007).
17. *Eprouvette Non Entaillée pour Essai de Résilience*, Norme ISO 5754 (1978).
18. *Détermination de la Résistance à la Rupture Transversale*, Norme ISO 3325 (1996).
19. C. Ionici and D. Dobrota, *Science of Sintering*, **45,** No. 1: 21 (2013).
20. S. M. Habibi, K. Janghorban, H. Khorsand, and S. A. J. Jahromi, *Proc. 3rd International Powder Metallurgy Conference* (Ankara: Turkish Powder Metallurgy Association: 2002), p. 398.
21. E. Dudrova, M. Kabatova, R. Bidulsky, and A. S. Wronski, *Powder Metallurgy*, **47**: 181 (2004).
22. *Steel Heat Treatment. Handbook* (Ed. G. E. Totten) (CRC Press: 2006).
23. *Höganas Handbook for Sintered Components. Design and Mechanical Properties* (Höganas: 2004).
24. *Höganas Handbook for Sintered Components. Production of Sintered Components* (Höganas: 2004).

25. A. Basu, J. Dutta Majumdar, J. Alphonsa, S. Mukherjee, and I. Manna, *Mater. Lett.*, **62:** 3117 (2008).
26. F. Chagnon and L. Tremblay, *World Congress and Exhibition* (Vienna: 2004).
27. W. M. De Silva, R. Binder, and J. D. B. de Mello, *Wear,* **258:** 166 (2005).
28. R. Hoffmann and K. H. Weissohn, *The Use of Oxygen Probes in Nitriding and Nitro-Carburizing*, No. 267: 39 (1993).
29. D. Ghiglione, C. Louroux, and C. Tournier, *Technique de L'ingénieur*, M1227 (2002).
30. H. C. Pavanati, G. Strafellini, A. M. Maliska, and A. N. Klein, *Wear,* **265:** 301 (2008).
31. N. Candela, F. Velasco, and J. M. Torralba, *Materials Science and Engineering A,* **259,** Iss. 1: 98 (1999).
32. P. Belkin, S. Kusmanov, A. Naumov, and Y. Parkaeva, *Adv. Mater. Res.*, **704:** 31 (2013).